Copyright Warning & Restrictions

The copyright law of the United States (Title 17, United States Code) governs the making of photocopies or other reproductions of copyrighted material.

Under certain conditions specified in the law, libraries and archives are authorized to furnish a photocopy or other reproduction. One of these specified conditions is that the photocopy or reproduction is not to be "used for any purpose other than private study, scholarship, or research." If a, user makes a request for, or later uses, a photocopy or reproduction for purposes in excess of "fair use" that user may be liable for copyright infringement,

This institution reserves the right to refuse to accept a copying order if, in its judgment, fulfillment of the order would involve violation of copyright law.

Please Note: The author retains the copyright while the New Jersey Institute of Technology reserves the right to distribute this thesis or dissertation

Printing note: If you do not wish to print this page, then select "Pages from: first page # to: last page #" on the print dialog screen

ABSTRACT

VALIDATION OF SOLAR FLARE FORECASTING & EVOLUTION OF MAGNETIC HELICITY OF TWO ACTIVE REGIONS

by
Qin Li

This thesis includes two components: (1) Validation of the NJIT flare-forecasting model that was established in recent years is carried out based on the statistical correlation between solar magnetic parameters and flare productivity of active regions (ARs). 378 ARs are examined, comparing observation with prediction. It is found that the accuracy rate to some extent decreases with the level of flares. (2) The temporal evolution of the relative magnetic helicity of two ARs, AR 11072 and 11158 is investigated. The former is flare-quiet while the latter is flare-productive over the 5-day observation period. It is found that for both regions, the shear-term is a predominant factor of magnetic helicity flux. The shear-term has the same sign as the emergence-term in both ARs. AR 11158 follows the "helicity hemispheric rule" (i.e., negative in the North hemisphere and positive in the South hemisphere), whereas AR 11072 does not.

VALIDATION OF SOLAR FLARE FORECASTING & EVOLUTION OF MAGNETIC HELICITY OF TWO ACTIVE REGIONS

by

Qin Li

A Dissertation
Submitted to the Faculty of
New Jersey Institute of Technology
in Partial Fulfillment of the Requirements for the Degree of
Master of Science in Applied Physics

Department of Physics

May 2013

APPROVAL PAGE

VALIDATION OF SOLAR FLARE FORECASTING & EVOLUTION OF MAGNETIC HELICITY OF TWO ACTIVE REGIONS

Qin Li

Dr. Ju Jing, Dissertation Co-Advisor — Date
Research Professor of Physics, NJIT

Dr. Haimin Wang, Dissertation Co-Advisor — Date
Distinguished Professor of Physics, NJIT

Dr. Jiang Tao Su, Committee Member — Date
Professor, National Astronomical Observatory of China

BIOGRAPHICAL SKETCH

Author: Qin Li

Degree: Master of Applied Physics

Date: May 2013

Undergraduate and Graduate Education:

- Master of Science in Applied Physics,
  New Jersey Institute of Technology, Newark, NJ, 2013

- Bachelor of Science in Applied Physics,
  Shanghai University, Shanghai, P. R. China, 2011

Major: Applied Physics

DEDICATION

I would like to dedicate this thesis to my parents, who support and encourage me in continuing my physics study all the way. I would also like to appreciate my friends Xin Miao and Clinton Lien for helping me spell check.

ACKNOWLEDGMENT

I wish to thank my adviser Dr. Haimin Wang for introducing me to the topic as well the support on the way. Furthermore I would like to express my gratitude to my supervisor Dr. Ju Jing for the useful remarks and engagement through the learning process of this master's thesis. Also, I would like to thank Shuo Wang, who has given me a lot of help on the software.

TABLE OF CONTENTS

CHAPTER 1

INTRODUCTION

1.1 Solar Flares & CMEs

Solar flares, usually occur in active regions around sunspots and may affect corona, chromosphere and photosphere. When solar flares are emitted from the surface of the sun, a large number of high-energy particles are heated and ejected nearly at the speed of light into the interplanetary space. These emitted particles travel through universe in the form of radiation, and spectrum spans from radio waves to gamma rays. Though the majority of these rays cannot be observed by naked eyes, they do have an impact on earth's atmosphere and human health.

Coronal mass ejections (CMEs) and solar flares are always found to be associated. CMEs and flares often occur simultaneously and they are believed to be the main causes of many geoeffective activities. One of the major differences between CMEs and solar flares is their spatial scale, CMEs are relatively much larger eruption of the corona and carry more high-energy particles into interplanetary space compared to solar flares. Solar flares are classified as C-, M- and X-classes according to the soft X-ray flux. The strongest X-class flares are more likely related to CMEs (Andrews 2003). Because of the difference of spatial scale and number of particles carried by them, CMEs are more likely to have a significant effect on human activities than solar flares. When CMEs reach earth, they cause a temporary disturbance of the Earth's magnetic field by setting off a geomagnetic storm. During geomagnetic storm, CMEs may disrupt satellites in orbit,

telecommunication & navigation systems, and even black out entire region through affecting the electrical power grids, which cause enormous economic and commercial losses in increasingly technological society. However, efficient flare-forecasting can provide a warning for high-energy particles which can reach 1 AU~20 minutes after ejection interacting with the earth (Georgoulis & Rust 2007). For example, keeping astronaut on a mission from radiation poisoning which is always carried by a flare or a CME.

1.2 Previous Work on Forecasting Model & Validation Purpose

NJIT group has a long tradition of developing techniques to predict solar flares. In previous research, the ordinal logistic regression method was utilized as a prediction model (Song et al, 2009), whereby the probability of C/M/X class flares in each active region during the next 1-day time period can be calculated. In this method, there're three core predictors, which are the total unsigned magnetic flux (T_{flux}), the length of the strong-gradient neutral line (L_{gnl}) and the total magnetic dissipation (E_{diss}). Eventually this method has been proven to be a simple and reasonable approach for flare prediction.

One of the main purposes of the thesis is to validate the forecasting results that are based on statistical study of helicity injection in 378 ARs. Validation results will help us to assess and improve the prediction model.

Solar active regions occupy smaller areas than quiet regions, but they produce the majority of solar activity in the form of flares and CMEs; they are considered as the main sources of flares as well due to the presence of intense magnetic fields. In the majority of

active regions, only subflaring activities exist. Magnetic energy and helicity are two essential factors to be studied regarding to the magnetic properties of active regions, and they clearly describe how energetic and complex an active region is. If the solar magnetic field can be divided into interior field and coronal field, the interaction between two fields depends on how magnetic helicity is transferred from one to another (Berger 1999). Further, the conservation of the helicity as a function of time can be observed once the electrical conductivity δ is set to infinity which resulting a zero value from dH/dt (Woltjer 1958).

1.3 Active Regions (ARs) & Magnetic Helicity

In this research, two different ARs present opposite characters toward the Hemisphere rule. The forming mechanism of "Hemisphere rule" may include differential rotation, effect of the Coriolis force, subsurface dynamo (Gilman & Charbonneau 1999) and the interaction of flux tubes vertically rising through the convection zone with helical convection turbulence. Differential rotation may occur in fluid due to its particular structure which may lead to different points of the sun with different latitude and longitude moving at different angular velocities in time. Coriolis force is a force formed as a result of object's rotation, whereby object's motion is deflected. Subsurface dynamo consists much complicated terms such as subsurface flow, subsurface magnetic field, etc.

Generally, magnetic helicity is defined in volume V for closed system:

$$H = \int_v A(t) \bullet B(t) dv \tag{1.1}$$

where B is the magnetic field, and A is the vector potential for such magnetic field. In a simple connected volume bounded by a magnetic surface, the integral is invariant to gauge transformations $A \to A + \nabla\psi$, where ψ is a single-valued derivable function of space and time (Démoulin 2002). However, in open system the volume of interest is not bounded by magnetic surface, Gauss linking numbers will no longer be defined (Berger 1999). Hence the total helicity cannot be defined either. In order to solve this issue, a more general form of magnetic helicity integral crossing surface S, which is suited for open system such as ARs (Berger&Field 1984, Finn&Antonsen 1985) was developed:

$$H = \int_V (A + A_p) \cdot (B - B_p) dV \tag{1.2}$$

For the potential field B_p, the classical gauge conditions are the following ones (Berger 1988):

$$\begin{aligned} &\nabla \cdot A_p|_v = 0 \\ &A_p \cdot \hat{n}|_s = 0 \\ &\nabla \times A_p = B_p \\ &\nabla \times A_p \cdot \hat{n} = B_n \end{aligned} \tag{1.3}$$

The time derivative of magnetic helicity H is expected because it may reveal information of both dissipation and transport across boundaries:

$$\frac{dH}{dt} = -2\int E \cdot B d^3x + 2\oint_s A_p \times E \cdot \hat{n}\, d^2x \tag{1.4}$$

Suppose $E = B \times V$,

Then the equation could be written in another form (Berger 1984):

$$\frac{dH}{dt} = 2\int_S (\overrightarrow{A_p} \cdot \overrightarrow{B_t}) V_n dS - 2\int_S (\overrightarrow{A_p} \cdot \overrightarrow{V_t}) B_n dS \qquad (1.5)$$

where the helicity is measured in terms of the vector potential A_p. B_n, B_t are normal and tangential magnetic field, V_n and V_t refer to the normal and tangential components of velocity V, respectively. Here V is the velocity perpendicular to magnetic field lines. The first term is defined as the emergence term while the second one is the shear term. There are two ways to describe the mechanism of magnetic helicity in corona. It either come from the twisted magnetic flux tubes emerging from the solar interior to outward (first term; emergence-term hereafter), or from shearing and braiding the field lines on the solar surface (second term; shear-term hereafter) (Liu & Schuck 2012).

By using local correlation tracking (LCT) velocity, the shear-term can be derived:

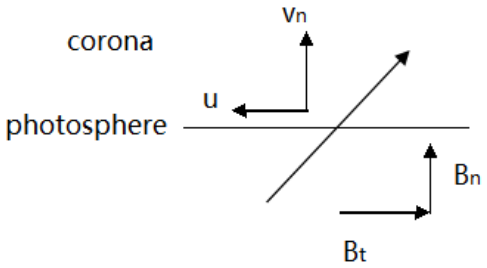

Figure.1 V_n is the vertical motion velocity, B_n and B_t respectively refer to normal and tangential components of magnetic field, u is the flux transport velocity.

In Fig.1, the LCT velocity is: $u = u_t - \frac{v_n}{B_n} B_t$, therefore (Démoulin 2003):

$$\frac{dH}{dt} = -2\int_s (A_p \cdot u) B_n d^2 x \qquad (1.6)$$

For some special modules such as rotating tube, it's difficult to solve it with LCT velocity, which will be explained in Chapter 3.

CHAPTER 2

DATA SETS

The data in this thesis all come from Helioseismic and Magnetic Imager (HMI) of Solar Dynamics Observatory (SDO), which is designed to study oscillation and the magnetic field on the solar surface.

The Solar Dynamics Observatory consists of three main instruments: Atmospheric Imaging Assembly (AIA), Extreme Ultraviolet variability Experiment (EVE) and Helioseismic and Magnetic Imager (HMI). AIA is designed to photograph the sun's surface and atmosphere in order to strengthen our understanding for the physical mechanism behind solar activity. EVE provides a direct method for scientists to measure fluctuations of the sun's ultraviolet irradiance, which may damage Earth's upper atmosphere through oxide desorption. The Helioseismic and Magnetic Imager (HMI) is accountable for mapping solar magnetic fields. The goal of SDO project is to investigate the magnetism of the sun (Pesnell 2012).

The HMI instrument is a filtergraph with a full disk coverage at 4096*4096 pixels, consisting of a telescope, polarization selector, an image stabilization system, a narrow band tunable filter and two cameras. It mainly provides four types of data: dopplergrams, continuum filtergrams, and both LOS and vector magnetograms (Vemareddy 2012). It helps us not only map solar magnetic fields but also establish the bridge between internal dynamo of the sun and solar activity on the surface. The observational data taken by the HMI with sufficient spatial and temporal resolution allow us to study magnetic energy

and helicity-injection into active-region corona, especially their buildup and evolution during flux emergence (Liu & Schuck 2012).

CHAPTER 3

TOOLS

IDL-a software system distributed by Exelis visual information solutions. Inc-is vectorized, numerical and interactive tool used for interactive processing of large amounts of data especially in space science area. It contains two-dimensional image data with accompanying pixel coordinate and spatial information, whereby the manipulation of image source can be transformed to the desired format.

The Solar Soft Ware (SSW) system is a set of integrated software libraries, databases and system utilities which provides a common programming and data analysis environment for solar physics. Primarily an IDL based system, SSW is a collection of common data management and analysis routines derived from the Yohkoh and SOHO missions, the Solar Data Analysis Center, the Astronomy libraries and other packages. The SSW environment is designed to provide a consistent look and feel for researchers (Freeland 1988).

The differential affine velocity estimator (DAVE; Schuck 2008) is developed to estimate velocities from line-of-sight magnetograms while its modified version (DAVE4VM; Schuck 2008) is used to estimate velocities from vector magnetogram. The vector velocity field in the photosphere is derived from the DAVE4VM that is applied to the time-series deprojected, registered vector magnetic field data (Liu & Schuck 2012). In most of previous studies, only the shear-term was considered. It is inevitable when those studies rely on line-of-sight tracking methods such as the local correlation tracking (LCT) or DAVE. These methods can only capture the apparent motion of magnetic

footpoints on the surface but are impotent to the vertical motion of magnetic flux (Schuck 2008). By contrast, DAVE4VM explicitly incorporates horizontal magnetic fields necessary for the description of vertical flows, and hence makes great progress in the estimates of vector velocity field on the photosphere. In this thesis, neither shear-term nor emergence-term can be ignored. Therefore DAVE4VM is used to carry out the calculation of the plasma velocity.

CHAPTER 4

VALIDATION OF FLARE-FORECASTING MODEL

Forecasting model plays a key role in space weather area, especially when trying to search a quick answer among small range of observational data. The predictive ability of flare-forecasting model determines if it is trustable, whereby the correct reaction could be carried out to prevent harmful CMEs from ejecting into earth's atmosphere without any warning.

A validation method has been presented to evaluate ordinal logistic regression method, which has been selected to be our main flare-forecasting model on previous predicting work. Fig.2 shows the histogram of data from the total number of observed events and theoretically predicted events from May, 2011 to August, 2012. X-axis stands for probabilistic confidence intervals of C/M/X-class flare. Y-axis shows the number of times the corresponding events occurred during observational period. Black rectangles refer to the observed events while red ones represent predicted events that are expected to equal to observed ones (disharmony events have been removed).

In statistics, the method of confidence intervals has been widely used because it provides a perfect visual illustration of the uncertainty level. In Fig.2, the probability of flares has been separated into ten confidence intervals. That 10% per interval suggested in histogram has a moderate level of uncertainty.

In this validation method, the validation number is defined as one when the level and time of an ejected flare are the same as predicted counterpart. Otherwise it is zero

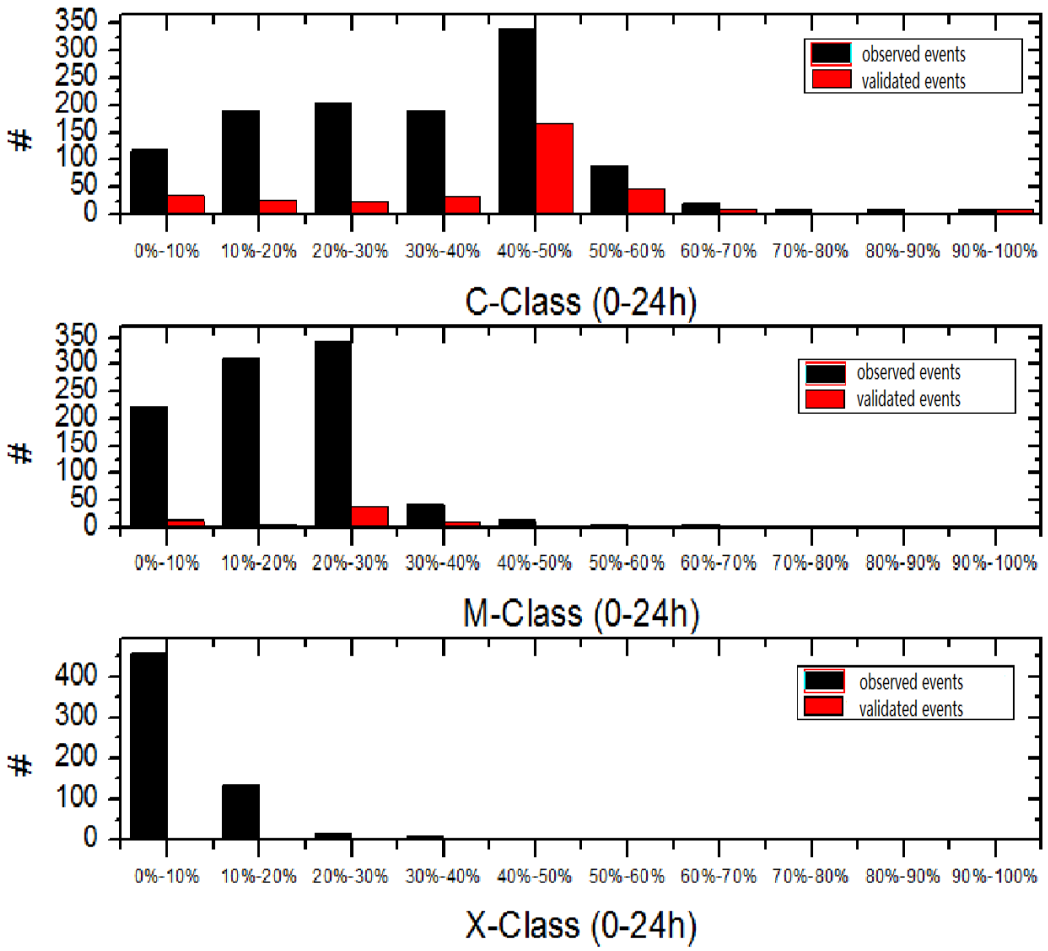

Figure. 2: Comparison of number of flaring events observed (black) and number of solar flaring events verified (red).

and cannot be considered into the total validation number. In addition, if the number of active region where the flare has been proved occurred does not correspond to the predicted number of active region, it cannot be added into validation number either. Then the predictive probability of each class equals to the ratio between number of validated events and the total number of observed events.

Here is the method to calculate the validation of predicted solar flare activity in the term of mathematical formula:

$$P = \frac{\sum_{i=1} V_i}{N}, \; V_i = \delta(X_j\text{-}X_k). \qquad (4.7)$$

where V_i stands for validation number, X_k represents each predicted case while X_j is observed event. If X_j is agree with X_k, the output of δ function is one. The p value is the probability expected to be similar to the predicted probability, assuming the estimated model is flawless. Also, it can be regarded as the ratio between the number of validated events and the total number of observed ones. This is agree with the significance of the statistical p-value which is "the probability of starting a test statistic at least as extreme as the observed events, assuming the null hypothesis is true." Thus, the output about predictive ability of the examined model is based on the comparison between the p value and the chosen uncertainty level. Summing the P values in the chosen uncertainty level may be good enough to decide the predictive ability of the model.

According to Fig. 2 & Table. 1, X-class flare prediction has the lowest accuracy of prediction among all of three flare levels. It is probably because of lacking number of sample events. By contrast, for C/M-class flare, the results of prediction have moderate accuracy. Moreover, nearly half results of the probability in C-class fit the confidence intervals, and all low confidence intervals fit them as well. It illustrates that the model still has reasonable forecasting capability, especially for low level of flares. In conclusion, the accuracy rate to some extent decreases with the level of flares.

Table.1 This is the direct comparison between expected certainty level and the real probability corresponding to observed events and predicted ones.

Observation / Forecasting	C	M	X
0%-10%	30. 66%	5. 82%	0. 88%
10%-20%	13. 68%	1. 28%	2. 99%
20%-30%	11. 76%	10. 82%	5. 88%
30%-40%	17. 37%	23. 26%	
40%-50%	49. 26%	7. 69%	
50%-60%	55. 06%	20. 00%	
60%-70%	52. 38%	20. 00%	
70%-80%		100%	
80%-90%	22. 22%		
90%-100%	100%		

Through the validation of C-class forecasting, the interval between 40%-60% based on largest number of estimated events has the mostly consistent predictive capability. Therefore, the earth could be prevented from impact of the same class flare more effectively in advance with a validated predictive model than without it. As a result of sun ramping up, solar flare activities forecasting becomes increasing accurate and applicable, especially for huge potentially dangerous and harmful space weather events. The continuous improvements for space weather forecasting cannot be alone without corresponding statistical validation.

CHAPTER 5

COMPARISON OF TWO ACTIVE REGIONS' (ARS) HELICITY BUDGETS

5.1 Two Emerging Active Regions (ARs): AR 11072 & AR 11158

Magnetic helicity budget, the best known index of topological complexity, measures twisting and linking fields (Moffat 1978, Berger & Field 1984). It is believed to play an important role in many areas of solar activity, for example, in coronal mass ejections (CMEs) (Rust 1994). If an active region field continues to build up helicity over time, the active region may lose stability, resulting in a mass ejection.

To study the magnetic helical properties in active regions around sunspots, two active regions (AR 11158 and AR 11072) have been analyzed. As one is notably flare-productive while another one is flare-quiet. AR 11072 emerged on 20 May 2010 at the S15E48, AR 11158 emerged on 10th February 2011 at the S20E60, which is more active than AR 11072. Both of them emerged quickly in a complex way, and generated several build-up flare with a strong horizontal flow. For AR 11072, less flare emerged during its disk passage.

5.2 AR 11072

The snapshots of normal magnetic field from 21th May for AR 11072 have been presented with the help of IDL software, which is shown in Fig.3. At the first stage there were two particles: black one was negative and white one was positive

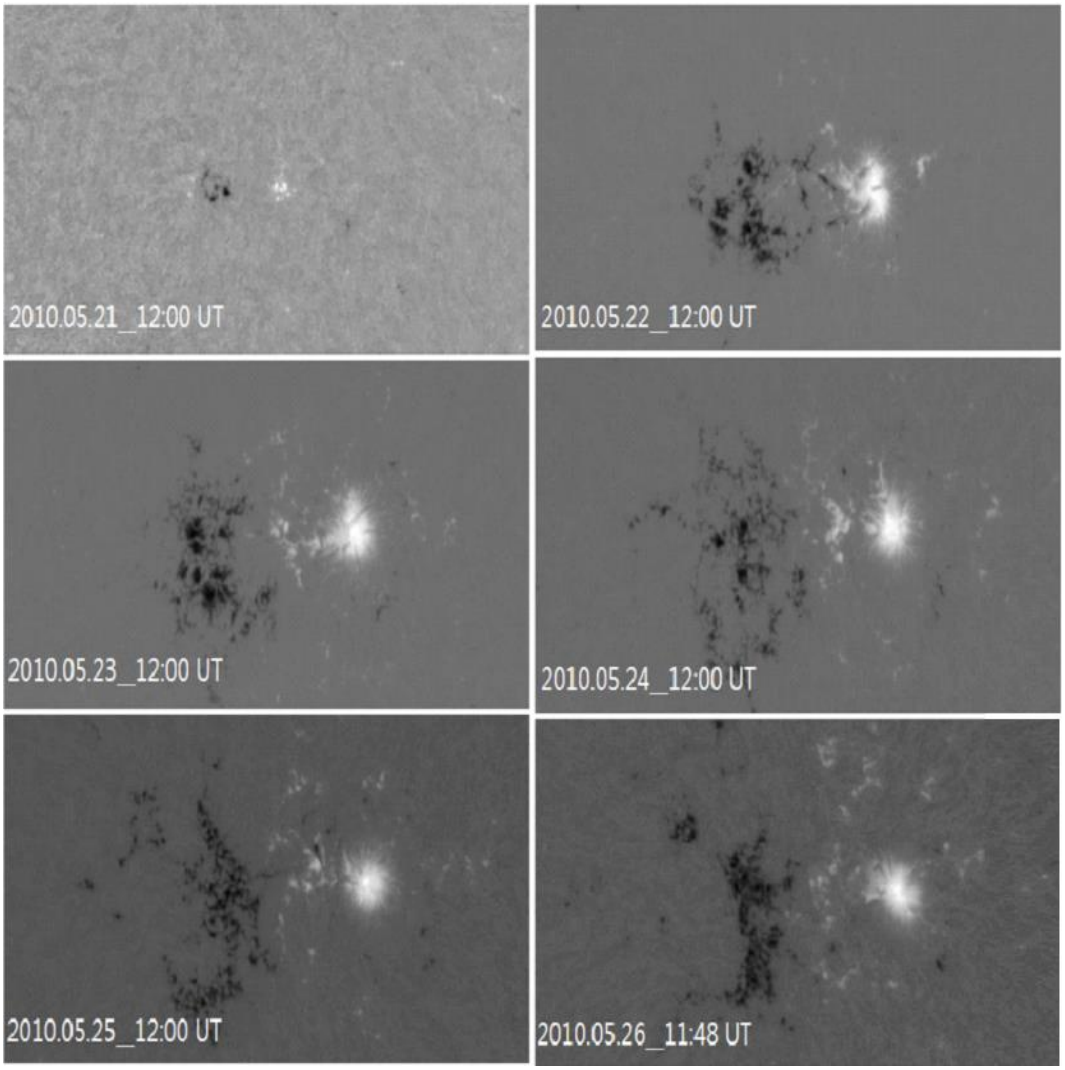

Figure. 3 Evolution of normal magnetic field of AR11072. White and black represent respectively to positive and negative fields.

field. No interaction occurred until they emerged, and afterward moved apart each other. Compact leading polarity (positive) and fragmented following polarity (negative) combining together developed a typical bipolar active region (Liu & Schuck 2012).

A helicity flux can be separated into two components contributed by two different velocities: one is horizontal velocity which is due to shearing and braiding the fields by photospheric shear motion; the other is vertical velocity that is due to vertical advection

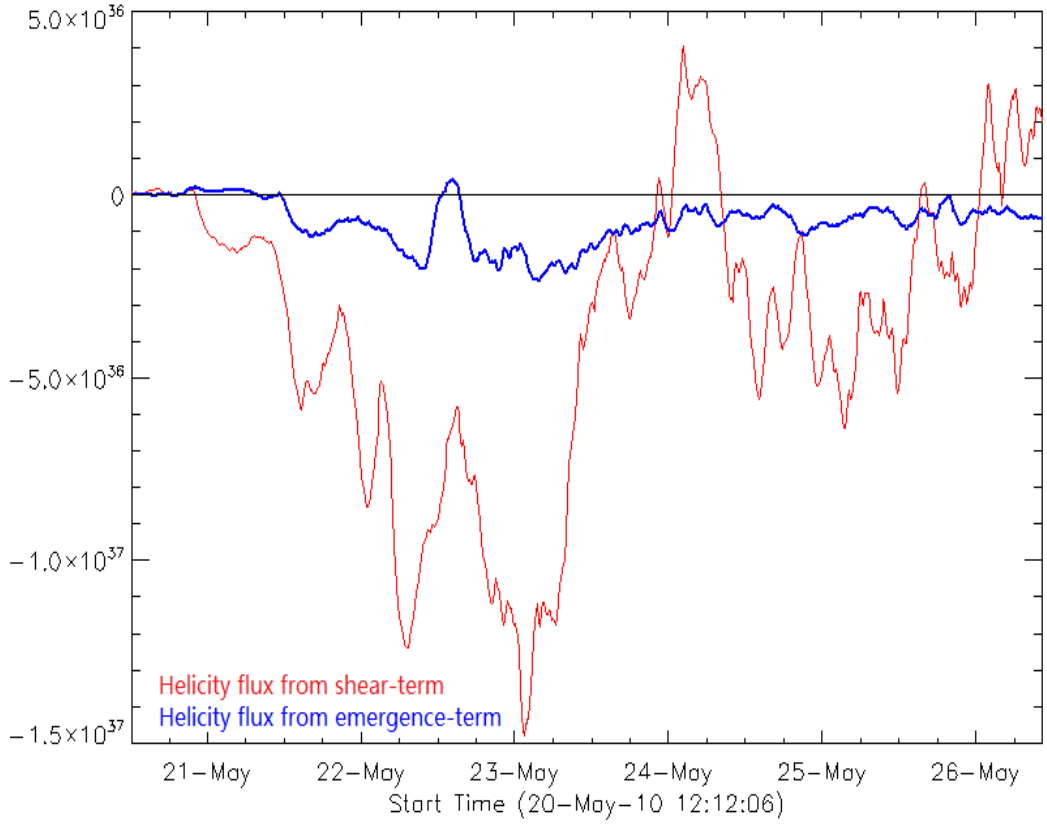

Figure. 4 Temporal profile of helicity flux across the photosphere from shear-term (blue line) and emergence-term (red line) for AR 11072, which was observed between 20th - 26th May, 2012.

of the twisted magnetic field across the photosphere. As shown in fig.4, this is temporal profile of helicity flux across the photosphere, from which there are red line and blue line which respectively represent shear and emergence term, separately due to V_t and V_n.

Fig.4 indicates that the shear-helicity flux acted more significantly than emergence-helicity flux during the days from 22-May to 24-May. Over the whole process emergence-helicity acted in a very moderate way that remained very low level consistently and no remarkable change showed up. The shear-term occupied the dominant place over the emergence- term from 21-May to 26-May. When flux emerged

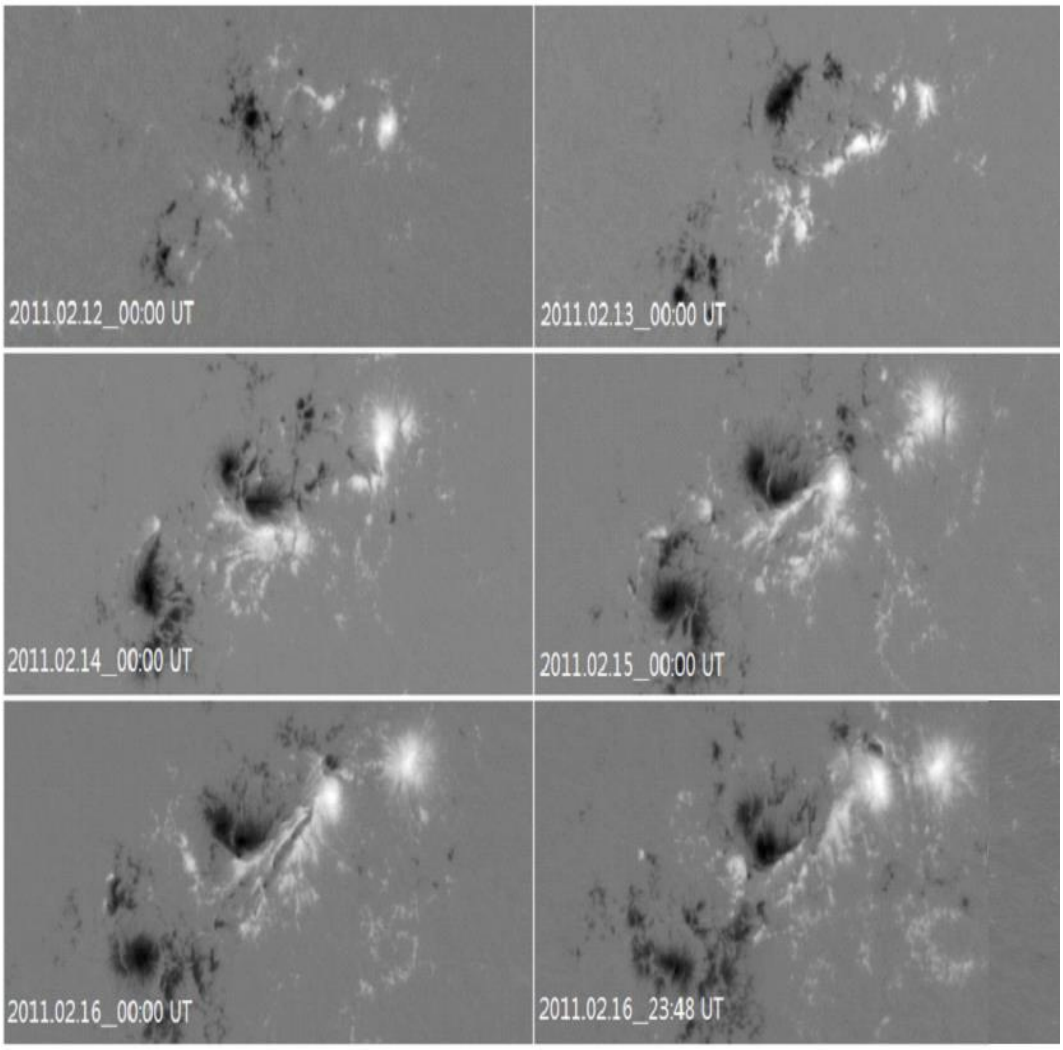

Figure. 5 Evolution of normal magnetic field of AR 11158. White and black represent respectively to positive and negative fields.

the shearing motion reached high quickly, afterward it tended to be zero when emergence stopped. Both of emergence-term and shear-term are negative, which is opposite to "hemisphere rule".

5.3AR 11158

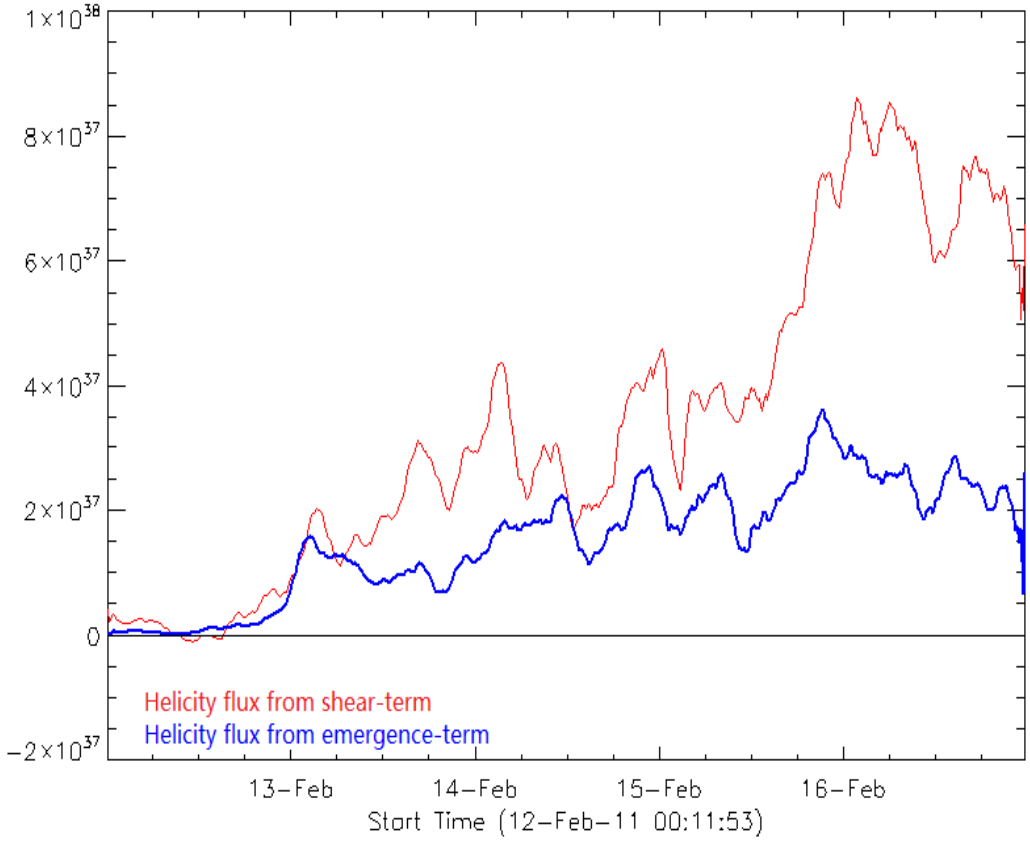

Figure. 6 Temporal profile of helicity flux across the photosphere from shear-term (blue line) and emergence-term (red line) for AR 11158, which was observed between 12th - 17th Feb, 2012.

Fig.5 shows evolution of normal magnetic field in AR 11158, which illustrates that it began to emerge at the first stage and never moved apart, at least from 12th Feb – 16th Feb. It turns out that AR 11158 is a multipolar active region, which was unlike the only existence of two opposite signed particles in AR 11072. One thing should be mentioned that highly twisted phenomenon at the center of negative field region probably can be contributed to the relatively fast self-rotation of sunspots.

Similarly as in Fig.3, temporal profile of helicity flux from shear-term and emergence-term is plotted in Fig.6. While both shear-helicity flux and emergence-helicity

flux were rising simultaneously from 12-Feb to 17-Feb, it is found that the shear-helicity flux dominated over the emergence-helicity. Evidently shear-helicity flux was injected more quickly than emergence-helicity flux. Obviously the so-called “hemispheric rule” has been obeyed that the patterns of both positive helicity occur predominantly in the southern solar atmosphere.

CHAPTER 6

CONCLUSIONS

A large proportion of validation work is attributed to the calculation through IDL software. Each correct couple of observed event and predicted event in 378 ARs has been considered into validation procedure. It is found that accuracy rate to some extent decreases with level of flares. In the C level, the interval between 40%-60% of solar-forecasting data is turned out to be the most accurate interval based on reality condition. The interval between 0%- 10% is highly agree with the low predictive probability in all three levels of flares. However, as lacking numbers of sample events in X level, except 0%-10%, the accuracy of other intervals from 10%-100% are controversial. Overall, our model still has reasonable forecasting capability, especially for C-class and low probabilistic intervals.

Secondly, the snapshots of normal magnetic field of AR 11172 and AR 11058 pose different evolutional trend. One acted as a typical bipolar active region and the other one acted as a multipolar system. Additionally, using HMI vector magnetic field data and calculating magnetic helicity, magnetic helicity of these two regions has been investigated. The helicity fluxes can be divided to two components. One is shearing and braiding the fields due to photospheric shear motion (shear-term) while the other from vertical advection of the twisted magnetic field (emergence-term) across the photosphere. During the entire emergence course, the shear-term and the emergence term of both ARs keep the same sign. In AR 11072 emergence motion is very small. However, in AR11158 both shear-term helicity and emergence-term rise up simultaneously, and equally

contribute to the helicity injection. In conclusion, it turns out that magnetic helicity in the corona is contributed mainly by the shear-helicity flux.

REFERENCES

Andrews, M. D. 2003, Solar Physics, 218, 261

Berger, M. A., & Field, G. B. 1984, J. Fluid Mechanics., 147, 13

Berger, Mitchell A. 1999, Plasma Physics and Controlled Fusion 41.12B: B167.

Berger, M. A. 1984, Geophysical & Astrophysical Fluid Dynamics, 30, 79

Démoulin et al.2002, P. 2007, Advances in Space Research, 39, 1674

Démoulin et al.2002, P., & Berger, M. A. 2003, Solar Physics, 215, 20

Freeland, S. L., and B. N. Handy 1998. Solar Physics 182.2: 497-500.

Finn, J. M., & Antonsen, T. M., Jr. 1985, Comments Plasma Physcis. Controlled Fusion,9,111

Georgoulis, Manolis K., and David M. Rust. The Astrophysical Journal Letters 661.1 (2007): L109.

Gilman, P. A., & Charbonneau, P. 1999, Geophysical Monograph Series, 111, 75

Kusano, K., Maeshiro, T., Yokoyama, T., & Sakurai, T. 2002, Astrophysical Journal. J., 577, 501

Liu, Y., and P. W. Schuck 2012. The Astrophysical Journal 761.2: 105.

Moffatt, H. K. 1978. Field Generation in Electrically Conducting Fluids. Cambridge University Press, Cambridge, London, New York, Melbourne.

Mason, J. P., and J. T. Hoeksema. 2010, The Astrophysical Journal 723.1: 634.

Nindos, A., Zhang, J., & Zhang, H. 2003, The Astrophysical Journal. J., 594, 1033

Pesnell, W. Dean, B. J. Thompson, and P. C. Chamberlin. 2012, Solar Physics 275.1-2 (2012): 3-1

Rust, D. M. 1994, Geophysical Research. Lett., 21, 241

Schuck, Peter W. The Astrophysical Journal 683.2 (2008): 1134

Woltjer, L. (1958). Proceedings of the National Academy Sciences 44(6): 489-491.